Proceedings of the 35th Chinese Control Conference
July 27-29, 2016, Chengdu, China

Adaptive Immersion and Invariance Based Control of Non-minimum Phase Hypersonic Vehicles

LIU Zhen, TAN Xiangmin, YUAN Ruyi, FAN Guoliang, YI Jianqiang

The Institute of Automation, Chinese Academy of Sciences, Beijing 100190
E-mail: liuzhen@ia.ac.cn

Abstract: A novel adaptive control design based on the immersion and invariance (I&I) theory is presented for the non-minimum phase hypersonic vehicles with parameter uncertainties. The vehicle dynamics are first divided into the velocity subsystem, the altitude/flight-path angle subsystem and the angle of attack/pitch rate subsystem. Then three I&I based adaptive controllers are designed for each subsystem respectively. The key feature of the proposed control scheme lies in the construction of the estimator, which can be used to assign prescribed dynamics to the estimate errors. The interaction of the flexible modes with the rigid dynamics is considered in both the synthesis of the controller and the analysis of the closed-loop system. A complete stability analysis of the closed-loop system is presented using Lyapunov theory. Simulation results show that the proposed control system provides precise and robust tracking of the velocity and altitude commands, as well as accurate regulation of angle of attack.

Key Words: Hypersonic vehicles, adaptive immersion and invariance, tracking control

1 Introduction

The nonlinear control problem associated with air-breathing hypersonic vehicles (AHSVs) has been discussed widely during the past decades. The main attraction of these vehicles resides in their significant potential in both military and civil applications [1-2]. Despite years of research, there are still many challenges for designing practical AHSV control systems.

Airframe-integrated engine configuration is widely preferred in AHSV, which yet results in strong interactions between the aerodynamics and the propulsion system. Considerable modeling uncertainty and dramatically varied aerodynamic characteristics also deserve special attention. Besides, the non-minimum phase behavior stemming from elevator-to-lift coupling and the significant flexible effects present further obstacles for control engineers [3-5].

Several results have been presented in the literature for the linearized versions of AHSV models [6-7]. But the design methods applied to the linearized AHSV models must be added with a step of gain scheduling, which increases the design complexity due to the extremely wide range of operating conditions. Feedback linearization method is widely used to avoid this problem [8-9], yet a precise vehicle model is needed. Furthermore, the vehicle angle of attack cannot be always guaranteed to a predetermined point in this way, which is negative for the operation of scramjet engines. Adaptive backstepping is applied to AHSV control system design in [10], based on the decomposition of the vehicle dynamics into velocity and altitude subsystems. Following the same architecture, many other adaptive control methods have been used in the literature [11-13]. But these traditional adaptive schemes generally design parameter update laws by careful cancelation of terms in the time-derivative of Lyapunov function, which can only ensure boundedness of the estimation errors, but hardly adjust the dynamical behavior of the errors [14]. Besides, several studies on distinct focuses of AHSV control design are reported as well [15-17]. A remarkable work among them is [15] which presents an nonlinear adaptive equivalent control based on interconnection subsystems for the non-minimum phase AHSV model. However, this inspired strategy neglects the flexible effects in both synthesis and analysis of the control system.

Immersion and invariance (I&I) theory is one of the latest advances in adaptive control [14]. This new method does not require knowledge of a Lyapunov function priorly when designing parameter adaptive laws. By adding a new term to the classical adaptive law, the dynamic behavior of the parameter estimate errors can be adjustable. This paper presents an adaptive I&I based control design for the AHSVs with parametric uncertainty. Benefiting from the convenience of stability analysis when using I&I method, the flexible effects on the vehicle dynamics are easily taken into account both in controller synthesis and analysis. The rest of this paper is organized as follows. The longitudinal model of AHSV and the control objective are presented in Section 2. The nonlinear controller for the AHSV model based on adaptive I&I theory is designed in Section 3, along with a complete analysis of the closed-loop system stability. Section 4 demonstrates the performance of the proposed control system via numerical simulations. Finally, conclusions are offered in Section 5.

2 Vehicle Model and Problem Formulation

The first-principle model (FPM) developed by [18] is used here. Its longitudinal dynamics can be expressed as

$$\dot{V} = (T\cos\alpha - D)/m - g\sin\gamma \tag{1}$$

$$\dot{h} = V\sin\gamma \tag{2}$$

$$\dot{\gamma} = (L + T\sin\alpha)/(mV) - g\cos\gamma/V \tag{3}$$

$$\dot{\alpha} = Q - \dot{\gamma} \tag{4}$$

$$\dot{Q} = M/I_{yy} \tag{5}$$

$$\ddot{\eta}_i = -2\zeta_i\omega_i\dot{\eta}_i - \omega_i^2\eta_i + N_i,\ \ i = 1,2,3 \tag{6}$$

*This work is supported by National Natural Science Foundation (NNSF) of China under Grants 61203003, 61421004, 61273149, and 61273336.

This model comprises five rigid-body state variables, namely, velocity V, altitude h, flight-path angle (FPA) γ, angle of attack (AOA) α and pitch rate Q, as well as six flexible states $\boldsymbol{\eta}=[\eta_1,\dot{\eta}_1,\eta_2,\dot{\eta}_2,\eta_3,\dot{\eta}_3]^T$ corresponding to the first three vibrational modes. The fuel equivalence ratio ϕ, elevator deflection δ_e and canard deflection δ_c are the control inputs, which affect (1)-(6) through the thrust T, lift L, drag D, pitch moment M and generalized forces N_i. The aerodynamic forces and moment, as well as the generalized forces are determined by AOA and the aerodynamic control surfaces, as described in [10]

$$T=\bar{q}S[C_{T,\phi}(\alpha)\phi+C_T(\alpha)+C_T^{\eta}\boldsymbol{\eta}] \tag{7}$$

$$L=\bar{q}SC_L(\alpha,\delta_e,\delta_c,\boldsymbol{\eta}) \tag{8}$$

$$D=\bar{q}SC_D(\alpha,\delta_e,\delta_c,\boldsymbol{\eta}) \tag{9}$$

$$M=z_TT+\bar{q}SC_M(\alpha,\delta_e,\delta_c,\boldsymbol{\eta}) \tag{10}$$

$$\begin{aligned}N_i=\bar{q}S[&N_i^{\alpha^2}\alpha^2+N_i^{\alpha}\alpha+N_i^{\delta_e}\delta_e\\&+N_i^{\delta_c}\delta_c+N_i^0+N_i^{\eta}\boldsymbol{\eta}],\quad i=1,2,3\end{aligned} \tag{11}$$

where the coefficients are expressed as

$$\begin{aligned}
&C_{T,\phi}(\alpha)=C_T^{\phi\alpha^3}\alpha^3+C_T^{\phi\alpha^2}\alpha^2+C_T^{\phi\alpha}\alpha+C_T^{\phi}\\
&C_T(\alpha)=C_T^3\alpha^3+C_T^2\alpha^2+C_T^1\alpha+C_T^0\\
&C_M(\alpha,\delta_e,\delta_c,\boldsymbol{\eta})=C_M^{\alpha^2}\alpha^2+C_M^{\alpha}\alpha+C_M^{\delta_e}\delta_e+C_M^{\delta_c}\delta_c+C_M^0+C_M^{\eta}\boldsymbol{\eta}\\
&C_L(\alpha,\delta_e,\delta_c,\boldsymbol{\eta})=C_L^{\alpha}\alpha+C_L^{\delta_e}\delta_e+C_L^{\delta_c}\delta_c+C_L^0+C_L^{\eta}\boldsymbol{\eta}\\
&C_D(\alpha,\delta_e,\delta_c,\boldsymbol{\eta})=C_D^{\alpha^2}\alpha^2+C_D^{\alpha}\alpha+C_D^{\delta_e^2}\delta_e^{\,2}+C_D^{\delta_e}\delta_e+C_D^{\delta_c^2}\delta_c^{\,2}\\
&\qquad\qquad+C_D^{\delta_c}\delta_c+C_D^0+C_D^{\eta}\boldsymbol{\eta}\\
&C_j^{\eta}=[C_j^{\eta 1},0,C_j^{\eta 2},0,C_j^{\eta 3},0],\ j=T,M,L,D\\
&N_i^{\eta}=[N_i^{\eta 1},0,N_i^{\eta 2},0,N_i^{\eta 3},0],\ j=1,2,3
\end{aligned} \tag{12}$$

Generally, there exist various uncertainties in AHSV model, especially for the aerodynamic coefficients. To present the robustness with respect of the model parameter uncertainties, all the aerodynamic coefficients of equation (12) are assumed to be unknown in this paper and a control system is designed under that assumption to achieve accurate tracking for the velocity and altitude commands, as well as precise regulation of angle of attack.

3 Adaptive Immersion and Invariance Based Controller Design

An adaptive I&I based controller for AHSV is derived in this section. The whole control system is divided into three subsystems, namely, the velocity subsystem, the altitude/FPA subsystem, and the AOA/pitch rate subsystem, as shown in Fig. 1. Motivated by [15], the terms related to the canard and elevator in both altitude/FPA subsystem and AOA/pitch rate subsystem are treated as two virtual control inputs, $\boldsymbol{E}_1$ and $\boldsymbol{E}_2$, respectively. Thus the relative degree between the output and the virtual control in each of the two subsystems is changed to two, which removes the zero-dynamics from the model. The actual deflections of elevator and canard can then be derived via $\boldsymbol{E}_1$ and $\boldsymbol{E}_2$.

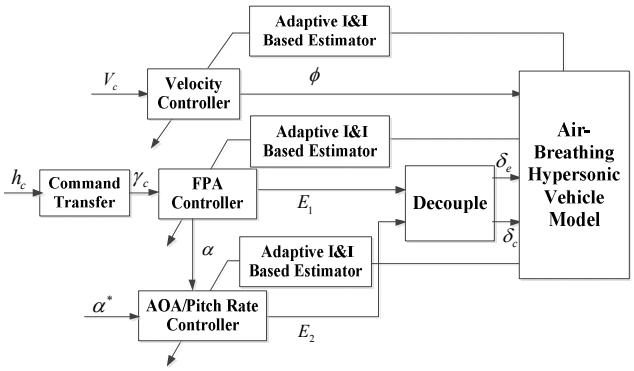

Fig. 1. The configuration of the whole control system

3.1 Controller for the Velocity Subsystem

The dynamics of $\tilde{V}=V-V_c$ can be written as

$$\dot{\tilde{V}}=\boldsymbol{F}_V^{\,T}\boldsymbol{\theta}_{V1}\phi+\boldsymbol{G}_V^{\,T}\boldsymbol{\theta}_{V2}-g\sin\gamma-\dot{V}_c+\bar{q}S(\boldsymbol{C}_{\boldsymbol{T}}^{\boldsymbol{\eta}}\cos\alpha-\boldsymbol{C}_{\boldsymbol{D}}^{\boldsymbol{\eta}})\tilde{\boldsymbol{\eta}}/m \tag{13}$$

where $\boldsymbol{\theta}_{V1}$ and $\boldsymbol{\theta}_{V2}$ are the vectors of unknown constant parameters, $\tilde{\boldsymbol{\eta}}=\boldsymbol{\eta}-\boldsymbol{\eta}^*$ with $\boldsymbol{\eta}^*$ steady flexible states of trim condition, and

$$\begin{aligned}
&\boldsymbol{F}_V=\bar{q}S\cos\alpha[\alpha^3,\alpha^2,\alpha,1]^T/m\\
&\boldsymbol{\theta}_{V1}=[C_T^{\phi\alpha^3},C_T^{\phi\alpha^2},C_T^{\phi\alpha},C_T^{\phi}]^T\\
&\boldsymbol{G}_V=\bar{q}S[\alpha^3\cos\alpha,\alpha^2\cos\alpha,\alpha\cos\alpha,\cos\alpha,-\alpha^2,-\alpha,-1,\cos\alpha,-1]^T/m\\
&\boldsymbol{\theta}_{V2}=[C_T^3,C_T^2,C_T^1,C_T^0,C_D^{\alpha^2},C_D^{\alpha},C_D^0,\boldsymbol{C}_{\boldsymbol{T}}^{\boldsymbol{\eta}}\boldsymbol{\eta}^*,\boldsymbol{C}_{\boldsymbol{D}}^{\boldsymbol{\eta}}\boldsymbol{\eta}^*]^T
\end{aligned}$$

According to adaptive I&I theory, the full estimates of $\boldsymbol{\theta}_{V1}$ and $\boldsymbol{\theta}_{V2}$ can be respectively defined as $\hat{\boldsymbol{\theta}}_{V1}+\boldsymbol{\beta}_{V1}$ and $\hat{\boldsymbol{\theta}}_{V2}+\boldsymbol{\beta}_{V2}$, where $\hat{\boldsymbol{\theta}}_{Vi}$ is generated by an update law $\dot{\hat{\boldsymbol{\theta}}}_{Vi}=\omega(\tilde{V},\hat{\boldsymbol{\theta}}_{Vi})$ and $\boldsymbol{\beta}_{Vi}$ is a nonlinear vector function to be determined. Notably a new term $\boldsymbol{\beta}_{Vi}$ is added to the estimates here. The advantage offered by this additional term will be shown in the following design. The estimate errors can then be written as

$$\boldsymbol{z}_V=\hat{\boldsymbol{\theta}}_V+\boldsymbol{\beta}_V-\boldsymbol{\theta}_V \tag{14}$$

where $\boldsymbol{z}_V=[\boldsymbol{z}_{V1}^{\,T},\boldsymbol{z}_{V2}^{\,T}]^T$, $\hat{\boldsymbol{\theta}}_V=[\hat{\boldsymbol{\theta}}_{V1}^{\,T},\hat{\boldsymbol{\theta}}_{V2}^{\,T}]^T$, $\boldsymbol{\beta}_V=[\boldsymbol{\beta}_{V1}^{\,T},\boldsymbol{\beta}_{V2}^{\,T}]^T$ and $\boldsymbol{\theta}_V=[\boldsymbol{\theta}_{V1}^{\,T},\boldsymbol{\theta}_{V2}^{\,T}]^T$.

The stabilizing signal ϕ can be chosen as

$$\boldsymbol{F}_V^{\,T}(\hat{\boldsymbol{\theta}}_{V1}+\boldsymbol{\beta}_{V1})\phi=-\boldsymbol{G}_V^{\,T}(\hat{\boldsymbol{\theta}}_{V2}+\boldsymbol{\beta}_{V2})+g\sin\gamma+\dot{V}_c-k_V\tilde{V} \tag{15}$$

where $k_V>0$. Substituting (15) into (13) yields

$$\dot{\tilde{V}}=-k_V\tilde{V}-\boldsymbol{\Phi}_V^{\,T}\boldsymbol{z}_V+(\bar{q}S/m)(\boldsymbol{C}_{\boldsymbol{T}}^{\boldsymbol{\eta}}\cos\alpha-\boldsymbol{C}_{\boldsymbol{D}}^{\boldsymbol{\eta}})\tilde{\boldsymbol{\eta}} \tag{16}$$

where $\boldsymbol{\Phi}_V=[\boldsymbol{F}_V^{\,T}\phi,\boldsymbol{G}_V^{\,T}]^T$.

Next consider the design of the parameter estimator. Differentiating (14) and then substituting (16) yield the dynamics of the estimate errors as

$$\dot{\boldsymbol{z}}_V=\dot{\hat{\boldsymbol{\theta}}}_V+\frac{\partial\boldsymbol{\beta}_V}{\partial\tilde{V}}(-k_V\tilde{V}-\boldsymbol{\Phi}_V^{\,T}\boldsymbol{z}_V+\frac{\bar{q}S}{m}(\boldsymbol{C}_{\boldsymbol{T}}^{\boldsymbol{\eta}}\cos\alpha-\boldsymbol{C}_{\boldsymbol{D}}^{\boldsymbol{\eta}})\tilde{\boldsymbol{\eta}}) \tag{17}$$

In view of (17), the update law $\dot{\hat{\boldsymbol{\theta}}}_V$ can be specified as

$$\dot{\hat{\boldsymbol{\theta}}}_V=\left(\partial\boldsymbol{\beta}_V/\partial\tilde{V}\right)(k_V\tilde{V}) \tag{18}$$

Then the dynamics of the estimate errors are changed into

$$\dot{z}_V = \left(\partial \boldsymbol{\beta}_V / \partial \tilde{V}\right)\left(-\boldsymbol{\Phi}_V^T z_V + \frac{\bar{q}S}{m}(\boldsymbol{C}_T^{\boldsymbol{\eta}} \cos\alpha - \boldsymbol{C}_D^{\boldsymbol{\eta}})\tilde{\boldsymbol{\eta}}\right) \quad (19)$$

Now $\boldsymbol{\beta}_V$ is chosen to drive the dynamics of z_V asymptotically to zero. The introduction of $\boldsymbol{\beta}_V$ allows construction of the z_V dynamics, which actually adds an extra degree of freedom in designing parameter estimator. One choice for $\boldsymbol{\beta}_V$ is

$$\partial \boldsymbol{\beta}_V / \partial \tilde{V} = \mathbf{r}_V \boldsymbol{\Phi}_V \quad (20)$$

where $\mathbf{r}_V = diag[r_{1V}\boldsymbol{I}_{4\times 4}, r_{2V}\boldsymbol{I}_{9\times 9}]$ and $r_{1V} > 0$, $r_{2V} > 0$. Substituting (20) into (19), we have

$$\dot{z}_V = -\mathbf{r}_V \boldsymbol{\Phi}_V \boldsymbol{\Phi}_V^T z_V + \mathbf{r}_V \boldsymbol{\Phi}_V \left(\bar{q}S/m\right)(\boldsymbol{C}_T^{\boldsymbol{\eta}} \cos\alpha - \boldsymbol{C}_D^{\boldsymbol{\eta}})\tilde{\boldsymbol{\eta}} \quad (21)$$

3.2 Controller for the Altitude/FPA Subsystem

The FPA command γ_c can be generated from the altitude command h_c by using

$$\gamma_c = -\arctan(k_h(h - h_c) + k_i \int (h - h_c)dt) \quad (22)$$

where $k_h > 0$ and $k_i > 0$.

Then the dynamics of $\tilde{\gamma} = \gamma - \gamma_c$ can be written as

$$\begin{aligned}\dot{\tilde{\gamma}} = {} & F_\gamma \theta_{\gamma 1}\alpha + \boldsymbol{G}_\gamma^T \boldsymbol{\theta}_{\gamma 2} - g\cos\gamma/V - \dot{\gamma}_c \\ & + \boldsymbol{E}_1^T \boldsymbol{\theta}_{\gamma 3} + F_\gamma(\boldsymbol{C}_T^{\boldsymbol{\eta}} \sin\alpha + \boldsymbol{C}_L^{\boldsymbol{\eta}})\tilde{\boldsymbol{\eta}}\end{aligned} \quad (23)$$

where $\theta_{\gamma 1}$, $\boldsymbol{\theta}_{\gamma 2}$ and $\boldsymbol{\theta}_{\gamma 3}$ are unknown parameters, $\boldsymbol{E}_1$ is the equivalent virtual control input for the altitude/FPA subsystem, and

$$F_\gamma = \bar{q}S/(mV), \quad \theta_{\gamma 1} = C_L^\alpha > 0$$

$$\boldsymbol{\theta}_{\gamma 2} = [C_T^{\phi\alpha^3}, C_T^{\phi\alpha^2}, C_T^{\phi\alpha}, C_T^{\phi}, C_T^3, C_T^2, C_T^1, C_T^0, \boldsymbol{C}_T^{\boldsymbol{\eta}}\boldsymbol{\eta}^*, C_L^0, \boldsymbol{C}_L^{\boldsymbol{\eta}}\boldsymbol{\eta}^*]^T$$

$$\begin{aligned}\boldsymbol{G}_\gamma = F_\gamma[& \alpha^3\phi\sin\alpha, \alpha^2\phi\sin\alpha, \alpha\phi\sin\alpha, \phi\sin\alpha, \\ & \alpha^3\sin\alpha, \alpha^2\sin\alpha, \alpha\sin\alpha, \sin\alpha, \sin\alpha, 1, 1]^T\end{aligned}$$

$$\boldsymbol{E}_1 = F_\gamma[\delta_e, \delta_c]^T, \quad \boldsymbol{\theta}_{\gamma 3} = [C_L^{\delta_e}, C_L^{\delta_c}]^T$$

Similarly to the design for the velocity subsystem, the full estimates of $\theta_{\gamma 1}$, $\boldsymbol{\theta}_{\gamma 2}$ and $\boldsymbol{\theta}_{\gamma 3}$ are defined as $\hat{\theta}_{\gamma 1} + \beta_{\gamma 1}$, $\hat{\boldsymbol{\theta}}_{\gamma 2} + \boldsymbol{\beta}_{\gamma 2}$ and $\hat{\boldsymbol{\theta}}_{\gamma 3} + \boldsymbol{\beta}_{\gamma 3}$, respectively. Then the estimate errors are given as

$$z_\gamma = \hat{\boldsymbol{\theta}}_\gamma + \boldsymbol{\beta}_\gamma - \boldsymbol{\theta}_\gamma \quad (24)$$

Next design the equivalent virtual control input $\boldsymbol{E}_1$ as

$$\begin{aligned}\boldsymbol{E}_1^T(\hat{\boldsymbol{\theta}}_{\gamma 3} + \boldsymbol{\beta}_{\gamma 3}) = {} & -F_\gamma(\hat{\theta}_{\gamma 1} + \beta_{\gamma 1})\alpha^* - \boldsymbol{G}_\gamma^T(\hat{\boldsymbol{\theta}}_{\gamma 2} + \boldsymbol{\beta}_{\gamma 2}) \\ & + g\cos\gamma/V + \dot{\gamma}_c - k_\gamma\tilde{\gamma}\end{aligned} \quad (25)$$

where $k_\gamma > 0$ and α^* is the desired trim value of AOA. Notably the value of α^* should be generated to satisfy an admissible range, which corresponds to the actual project of the scramjet engine. Substituting (25) into (23) yields

$$\begin{aligned}\dot{\tilde{\gamma}} = {} & -k_\gamma\tilde{\gamma} - \boldsymbol{G}_\gamma^T \boldsymbol{z}_{\gamma 2} - \boldsymbol{E}_1^T \boldsymbol{z}_{\gamma 3} - F_\gamma(\tilde{\theta}_{\gamma 1} + \beta_{\gamma 1})\alpha^* \\ & + F_\gamma\theta_{\gamma 1}\alpha + F_\gamma(\boldsymbol{C}_T^{\boldsymbol{\eta}} \sin\alpha + \boldsymbol{C}_L^{\boldsymbol{\eta}})\tilde{\boldsymbol{\eta}}\end{aligned} \quad (26)$$

Define the reference command for the angle of attack as $\alpha_c = \alpha^* - \tilde{\gamma}$ [10]. Considering the angle of attack tracking error $\tilde{\alpha} = \alpha - \alpha_c$, (26) can be changed into

$$\begin{aligned}\dot{\tilde{\gamma}} = {} & -k_\gamma\tilde{\gamma} - \boldsymbol{G}_\gamma^T \boldsymbol{z}_{\gamma 2} - \boldsymbol{E}_1^T \boldsymbol{z}_{\gamma 3} - F_\gamma z_{\gamma 1}\alpha^* \\ & + F_\gamma\theta_{\gamma 1}(\tilde{\alpha} - \tilde{\gamma}) + F_\gamma(\boldsymbol{C}_T^{\boldsymbol{\eta}} \sin\alpha + \boldsymbol{C}_L^{\boldsymbol{\eta}})\tilde{\boldsymbol{\eta}}\end{aligned} \quad (27)$$

Now the parameter estimates used in (25) are designed. Following the same procedure as the one in Section 3.1, the update law $\dot{\hat{\boldsymbol{\theta}}}_\gamma$ and the additional function $\boldsymbol{\beta}_\gamma$ can be selected

$$\dot{\hat{\boldsymbol{\theta}}}_\gamma = \left(\partial \boldsymbol{\beta}_\gamma / \partial \tilde{\gamma}\right)(k_\gamma\tilde{\gamma}), \qquad \partial \boldsymbol{\beta}_\gamma / \partial \tilde{\gamma} = \mathbf{r}_\gamma \boldsymbol{\Phi}_\gamma \quad (28)$$

where $\mathbf{r}_\gamma = diag[r_{1\gamma}, r_{2\gamma}\boldsymbol{I}_{11\times 11}, r_{3\gamma}\boldsymbol{I}_{2\times 2}]$, $\boldsymbol{\Phi}_\gamma = [F_\gamma\alpha^*, \boldsymbol{G}_\gamma^T, \boldsymbol{E}_1^T]^T$ and $r_{1\gamma} > 0$, $r_{2\gamma} > 0$, $r_{3\gamma} > 0$. Using (24) and (28) yields the dynamics of the estimate errors z_γ as

$$\begin{aligned}\dot{z}_\gamma = {} & -\mathbf{r}_\gamma \boldsymbol{\Phi}_\gamma \boldsymbol{\Phi}_\gamma^T z_\gamma + \mathbf{r}_\gamma \boldsymbol{\Phi}_\gamma F_\gamma \theta_{\gamma 1}(\tilde{\alpha} - \tilde{\gamma}) \\ & + \mathbf{r}_\gamma \boldsymbol{\Phi}_\gamma F_\gamma(\boldsymbol{C}_T^{\boldsymbol{\eta}} \sin\alpha + \boldsymbol{C}_L^{\boldsymbol{\eta}})\tilde{\boldsymbol{\eta}}\end{aligned} \quad (29)$$

With $\boldsymbol{\beta}_\gamma$ and $\hat{\boldsymbol{\theta}}_\gamma$ obtained from (28), the equivalent virtual control input $\boldsymbol{E}_1$ can be derived from (25).

3.3 Controller for the AOA/Pitch Rate Subsystem

The dynamics of AOA tracking error $\dot{\tilde{\alpha}}$ can be simply given as follow

$$\dot{\tilde{\alpha}} = q - \dot{\gamma}_c \quad (30)$$

For convenience, rewrite the dynamics of pitch rate from (5) and (12) as

$$\dot{q} = \boldsymbol{G}_q^T \boldsymbol{\theta}_{q2} + \boldsymbol{E}_2^T \boldsymbol{\theta}_{q3} + \left(\bar{q}S/I_y\right)(z_T\boldsymbol{C}_T^{\boldsymbol{\eta}} + \bar{c}\boldsymbol{C}_M^{\boldsymbol{\eta}})\tilde{\boldsymbol{\eta}} \quad (31)$$

where $\boldsymbol{\theta}_{q2}$ and $\boldsymbol{\theta}_{q3}$ are unknown parameters, $\boldsymbol{E}_2$ is the equivalent virtual control input for the AOA/pitch rate subsystem, and

$$\begin{aligned}\boldsymbol{G}_q = {} & \bar{q}S\bar{c}[\phi z_T\alpha^3, \phi z_T\alpha^2, \phi z_T\alpha, \phi z_T, z_T\alpha^3, \\ & z_T\alpha^2, z_T\alpha, z_T, z_T, \bar{c}\alpha^2, \bar{c}\alpha, \bar{c}, \bar{c}]^T / I_y\end{aligned}$$

$$\begin{aligned}\boldsymbol{\theta}_{q2} = {} & [C_T^{\phi\alpha^3}, C_T^{\phi\alpha^2}, C_T^{\phi\alpha}, C_T^{\phi}, C_T^3, C_T^2, C_T^1, C_T^0, \\ & \boldsymbol{C}_T^{\boldsymbol{\eta}}\boldsymbol{\eta}^*, C_M^{\alpha^2}, C_M^{\alpha}, C_M^0, \boldsymbol{C}_M^{\boldsymbol{\eta}}\boldsymbol{\eta}^*]^T\end{aligned}$$

$$\boldsymbol{E}_2 = \bar{q}S\bar{c}[\delta_e, \delta_c]^T / I_y$$

$$\boldsymbol{\theta}_{q3} = [C_M^{\delta_e}, C_M^{\delta_c}]^T$$

Introduce a surface as follow

$$S_{\alpha-q} = \dot{\tilde{\alpha}} + \lambda\tilde{\alpha} \quad (32)$$

Notably if $S_{\alpha-q} = 0$, it follows that the AOA tracking error $\tilde{\alpha}$ converges to zero. Differentiating (32) yields

$$\begin{aligned}\dot{S}_{\alpha-q} = {} & \boldsymbol{G}_q^T \boldsymbol{\theta}_{q2} + \boldsymbol{E}_2^T \boldsymbol{\theta}_{q3} + \lambda q - \lambda\dot{\gamma}_c - \ddot{\gamma}_c \\ & + \left(\bar{q}S/I_y\right)(z_T\boldsymbol{C}_T^{\boldsymbol{\eta}} + \bar{c}\boldsymbol{C}_M^{\boldsymbol{\eta}})\tilde{\boldsymbol{\eta}}\end{aligned} \quad (33)$$

Define the estimates of $\boldsymbol{\theta}_{q2}$ and $\boldsymbol{\theta}_{q3}$ are $\hat{\boldsymbol{\theta}}_{q2} + \boldsymbol{\beta}_{q2}$ and $\hat{\boldsymbol{\theta}}_{q3} + \boldsymbol{\beta}_{q3}$, respectively. The estimate errors are

$$z_q = \hat{\boldsymbol{\theta}}_q + \boldsymbol{\beta}_q - \boldsymbol{\theta}_q \quad (34)$$

In view of (33), $\boldsymbol{E}_2$ can be defined as

$$\begin{aligned}\boldsymbol{E}_2^T(\hat{\boldsymbol{\theta}}_{q3} + \boldsymbol{\beta}_{q3}) = {} & -\boldsymbol{G}_q^T(\hat{\boldsymbol{\theta}}_{q2} + \boldsymbol{\beta}_{q2}) - \lambda q + \lambda\dot{\gamma}_c \\ & + \ddot{\gamma}_c - k_{\alpha-q}S_{\alpha-q} - \tilde{\alpha}\end{aligned} \quad (35)$$

where $k_{\alpha-q} > 0$. Substituting (35) into (33) yields

$$\dot{S}_{\alpha-q} = -k_{\alpha-q}S_{\alpha-q} - \boldsymbol{\Phi}_q^T \boldsymbol{z}_q - \tilde{\alpha} + \frac{\bar{q}S}{I_y}(z_T\boldsymbol{C}_T^{\boldsymbol{\eta}} + \bar{c}\boldsymbol{C}_M^{\boldsymbol{\eta}})\tilde{\boldsymbol{\eta}} \quad (36)$$

where $\boldsymbol{\Phi}_q = [\boldsymbol{G}_q^T, \boldsymbol{E}_2^T]^T$.

Next design the parameter estimates $\hat{\boldsymbol{\theta}}_{q2}+\boldsymbol{\beta}_{q2}$ and $\hat{\boldsymbol{\theta}}_{q3}+\boldsymbol{\beta}_{q3}$. As Section 3.1, the update law $\dot{\hat{\boldsymbol{\theta}}}_q$ and the additional function $\boldsymbol{\beta}_q$ can be selected as

$$\dot{\hat{\boldsymbol{\theta}}}_q=\left(\partial\boldsymbol{\beta}_q/\partial S_{\alpha-q}\right)(k_{\alpha-q}S_{\alpha-q}+\tilde{\alpha}),\partial\boldsymbol{\beta}_q/\partial S_{\alpha-q}=\mathbf{r}_q\boldsymbol{\Phi}_q \quad (37)$$

where $\mathbf{r}_q=diag[r_{2q}\boldsymbol{I}_{13\times13},r_{3q}\boldsymbol{I}_{2\times2}]$ and $r_{2q}>0$, $r_{3q}>0$. Substituting (34) and (38) yields

$$\dot{z}_q=-\mathbf{r}_q\boldsymbol{\Phi}_q\boldsymbol{\Phi}_q^T z_q+\mathbf{r}_q\boldsymbol{\Phi}_q\left(\bar{q}S/I_y\right)(z_T\boldsymbol{C}_T^{\eta}+\bar{c}\boldsymbol{C}_M^{\eta})\tilde{\boldsymbol{\eta}} \quad (38)$$

With $\dot{\hat{\boldsymbol{\theta}}}_q$ and $\boldsymbol{\beta}_q$ from (37), the equivalent virtual control input $\boldsymbol{E}_2$ can be obtained from (35). Finally the deflections of elevator and canard can be derived from $\boldsymbol{E}_1$ and $\boldsymbol{E}_2$.

3.4 Stability Analysis for the Closed-Loop System

Rewrite the rigid-body dynamics of the closed-loop system

$$\begin{cases}\dot{\tilde{V}}=-k_V\tilde{V}-\boldsymbol{\Phi}_V^T z_V+\bar{q}S(\boldsymbol{C}_T^{\eta}\cos\alpha-\boldsymbol{C}_D^{\eta})\tilde{\boldsymbol{\eta}}/m\\ \dot{z}_V=-\mathbf{r}_V\boldsymbol{\Phi}_V\boldsymbol{\Phi}_V^T z_V+\bar{q}S\mathbf{r}_V\boldsymbol{\Phi}_V(\boldsymbol{C}_T^{\eta}\cos\alpha-\boldsymbol{C}_D^{\eta})\tilde{\boldsymbol{\eta}}/m\\ \dot{\tilde{\gamma}}=-k_\gamma\tilde{\gamma}-\boldsymbol{\Phi}_\gamma^T z_\gamma+F_\gamma\theta_{\gamma1}(\tilde{\alpha}-\tilde{\gamma})+F_\gamma(\boldsymbol{C}_T^{\eta}\sin\alpha+\boldsymbol{C}_L^{\eta})\tilde{\boldsymbol{\eta}}\\ \dot{z}_\gamma=-\mathbf{r}_\gamma\boldsymbol{\Phi}_\gamma\boldsymbol{\Phi}_\gamma^T z_\gamma+\mathbf{r}_\gamma\boldsymbol{\Phi}_\gamma F_\gamma\theta_{\gamma1}(\tilde{\alpha}-\tilde{\gamma})+\mathbf{r}_\gamma\boldsymbol{\Phi}_\gamma F_\gamma(\boldsymbol{C}_T^{\eta}\sin\alpha+\boldsymbol{C}_L^{\eta})\tilde{\boldsymbol{\eta}}\\ \dot{\tilde{\alpha}}=S_{\alpha-q}-\lambda\tilde{\alpha}\\ \dot{S}_{\alpha-q}=-k_{\alpha-q}S_{\alpha-q}-\boldsymbol{\Phi}_q^T z_q-\tilde{\alpha}+\bar{q}S(z_T\boldsymbol{C}_T^{\eta}+\bar{c}\boldsymbol{C}_M^{\eta})\tilde{\boldsymbol{\eta}}/I_y\\ \dot{z}_q=-\mathbf{r}_q\boldsymbol{\Phi}_q\boldsymbol{\Phi}_q^T z_q+\bar{q}S\mathbf{r}_q\boldsymbol{\Phi}_q(z_T\boldsymbol{C}_T^{\eta}+\bar{c}\boldsymbol{C}_M^{\eta})\tilde{\boldsymbol{\eta}}/I_y\end{cases} \quad (39)$$

According to [10], the stability analysis for the flexible states at the point $\boldsymbol{\eta}=\boldsymbol{\eta}^*$ can be converted into that at the origin for the following system

$$\dot{\tilde{\boldsymbol{\eta}}}=(\mathbf{A}_{\eta1}+\mathbf{A}_{\eta2})\boldsymbol{\eta}+\boldsymbol{B}_1\tilde{\gamma}+\boldsymbol{B}_2\tilde{\alpha} \quad (40)$$

where $\mathbf{A}_{\eta1}$, $\mathbf{A}_{\eta2}$, $\boldsymbol{B}_1$ and $\boldsymbol{B}_2$ can be obtained from [10]. Particularly, there exists a positive-definite matrix $\mathbf{Q}$ satisfying $\mathbf{Q}\mathbf{A}_{\eta1}+\mathbf{A}_{\eta1}^T\mathbf{Q}=-\mathbf{I}_{6\times6}$ for $\mathbf{A}_{\eta1}$ is a Hurwitz matrix, and the matrix $\bar{\mathbf{P}}=\mathbf{I}_{6\times6}-(\mathbf{Q}\mathbf{A}_{\eta2}+\mathbf{A}_{\eta2}^T\mathbf{Q})$ is also positive-definite for each element of $\mathbf{A}_{\eta2}$ is small enough in the AHSV flight envelope [10]. Therefore, the dynamics of the overall closed-loop system can be established by (39) and (40).

Assumption 1: The actual velocity value is bounded for the physical limits of the engine thrust, which also guarantees the boundedness of the related term $F_\gamma\theta_{\gamma1}=\bar{q}S\theta_{\gamma1}/(mV)$.

Theorem 1: Consider the system given by (39) and (40), and such that Assumption 1hold. Then there exist adaptive control laws described in Section 3, which guarantee the errors $\tilde{\boldsymbol{x}}=[\tilde{V},\boldsymbol{\Phi}_V^T z_V,\tilde{\gamma},\boldsymbol{\Phi}_\gamma^T z_\gamma,\tilde{\alpha},S_{\alpha-q},\boldsymbol{\Phi}_q^T z_q,\tilde{\boldsymbol{\eta}}^T]^T$ converge to zero asymptotically as the time tends to infinity, i.e., $\lim_{t\to\infty}\tilde{\boldsymbol{x}}=\mathbf{0}$, with all signals bounded.

Proof: Consider the following Lyapunov candidate function

$$\begin{aligned}W=&\frac{1}{2}\tilde{V}^2+\frac{1}{2}k_V^{-1}z_V^T\mathbf{r}_V^{-1}z_V+\frac{1}{2}\tilde{\gamma}^2+\frac{1}{2}z_\gamma^T\mathbf{r}_\gamma^{-1}z_\gamma+\frac{1}{2}\sigma_2\tilde{\alpha}^2\\&+\frac{1}{2}\sigma_2S_{\alpha-q}^2+\frac{1}{2}\sigma_2k_{\alpha-q}^{-1}z_q^T\mathbf{r}_q^{-1}z_q+\sigma_\eta\tilde{\boldsymbol{\eta}}^T\mathbf{Q}\tilde{\boldsymbol{\eta}}\end{aligned} \quad (41)$$

where $\sigma_2>0$, $\sigma_\eta>0$. Differentiating (41) along the trajectories of (39) and (40) yields

$$\begin{aligned}\dot{W}=&-k_V\tilde{V}^2-\boldsymbol{\Phi}_V^T z_V\tilde{V}-k_V^{-1}\left|\boldsymbol{\Phi}_V^T z_V\right|^2-(k_\gamma+F_\gamma\theta_{\gamma1})\tilde{\gamma}^2\\&-\left|\boldsymbol{\Phi}_\gamma^T z_\gamma\right|^2-(1+F_\gamma\theta_{\gamma1})\boldsymbol{\Phi}_\gamma^T z_\gamma\tilde{\gamma}+F_\gamma\theta_{\gamma1}\tilde{\gamma}\tilde{\alpha}+F_\gamma\theta_{\gamma1}\boldsymbol{\Phi}_\gamma^T z_\gamma\tilde{\alpha}\\&+\sigma_2[-\lambda\tilde{\alpha}^2-\boldsymbol{\Phi}_q^T z_qS_{\alpha-q}-k_{\alpha-q}S_{\alpha-q}^2-k_{\alpha-q}^{-1}\left|\boldsymbol{\Phi}_q^T z_q\right|^2]\\&+\tilde{V}\boldsymbol{C}_1\tilde{\boldsymbol{\eta}}+\boldsymbol{\Phi}_V^T z_V\boldsymbol{C}_1\tilde{\boldsymbol{\eta}}+\tilde{\gamma}\boldsymbol{C}_2\tilde{\boldsymbol{\eta}}+\boldsymbol{\Phi}_\gamma^T z_\gamma\boldsymbol{C}_2\tilde{\boldsymbol{\eta}}+S_{\alpha-q}\boldsymbol{C}_3\tilde{\boldsymbol{\eta}}\\&+\boldsymbol{\Phi}_q^T z_q\boldsymbol{C}_3\tilde{\boldsymbol{\eta}}-\sigma_\eta\tilde{\boldsymbol{\eta}}^T\bar{\mathbf{P}}\tilde{\boldsymbol{\eta}}+2\sigma_\eta\tilde{\boldsymbol{\eta}}^T\mathbf{Q}\boldsymbol{B}_1\tilde{\gamma}+2\sigma_\eta\tilde{\boldsymbol{\eta}}^T\mathbf{Q}\boldsymbol{B}_2\tilde{\alpha}\end{aligned}$$

where

$\boldsymbol{C}_1=\bar{q}S(\boldsymbol{C}_T^{\eta}\cos\alpha-\boldsymbol{C}_D^{\eta})/m$, $\boldsymbol{C}_2=F_\gamma(\boldsymbol{C}_T^{\eta}\sin\alpha+\boldsymbol{C}_L^{\eta})$, $\boldsymbol{C}_3=\bar{q}S(z_T\boldsymbol{C}_T^{\eta}+\bar{c}\boldsymbol{C}_M^{\eta})/I_y$ are used for notational convenience.

Then by Young's inequality, we have

$$\dot{W}\le-\tilde{\boldsymbol{x}}^T\mathbf{P}\tilde{\boldsymbol{x}} \quad (42)$$

where $\sigma_1>0$ and

$$\mathbf{P}=\left[\begin{array}{ccccccc|c}\frac{k_V}{2}&0&0&0&0&0&0&-\frac{\boldsymbol{C}_1}{2}\\0&\frac{1}{2k_V}&0&0&0&0&0&-\frac{\boldsymbol{C}_1}{2}\\0&0&\frac{2k_\gamma+F_\gamma\theta_{\gamma1}(2-\sigma_1)-\sigma_1}{2}&0&-\frac{F_\gamma\theta_{\gamma1}}{2}&0&0&(-\frac{\boldsymbol{C}_1^T}{2}-\sigma_\eta\mathbf{Q}\boldsymbol{B}_1)^T\\0&0&0&\frac{2\sigma_1-1-F_\gamma\theta_{\gamma1}}{2\sigma_1}&-\frac{F_\gamma\theta_{\gamma1}}{2}&0&0&-\frac{\boldsymbol{C}_1}{2}\\0&0&-\frac{F_\gamma\theta_{\gamma1}}{2}&-\frac{F_\gamma\theta_{\gamma1}}{2}&\lambda\sigma_2&0&0&\sigma_\eta\boldsymbol{B}_2^T\mathbf{Q}\\0&0&0&0&0&\frac{\sigma_2k_{\alpha-q}}{2}&0&-\frac{\boldsymbol{C}_2}{2}\\0&0&0&0&0&0&\frac{\sigma_2}{2k_{\alpha-q}}&-\frac{\boldsymbol{C}_2}{2}\\\hline-\frac{\boldsymbol{C}_1^T}{2}&-\frac{\boldsymbol{C}_1^T}{2}&-\frac{\boldsymbol{C}_1^T}{2}-\sigma_\eta\mathbf{Q}\boldsymbol{B}_1&-\frac{\boldsymbol{C}_1^T}{2}&-\sigma_\eta\mathbf{Q}\boldsymbol{B}_2&-\frac{\boldsymbol{C}_2^T}{2}&-\frac{\boldsymbol{C}_2^T}{2}&\sigma_\eta\bar{\mathbf{P}}\end{array}\right]$$

Let Δ_i denote the i-th order leading principal minor of $\mathbf{P}$. Obviously Δ_1 and Δ_2 are both positive. For

$$\Delta_3 = \frac{1}{4}[k_\gamma + F_\gamma\theta_{\gamma 1} - \frac{1}{2}\sigma_1(1+F_\gamma\theta_{\gamma 1})],$$

$$\Delta_4 = [1-\frac{1}{2}\sigma_1^{-1}(1+F_\gamma\theta_{\gamma 1})]\Delta_3,$$

there exist $k_\gamma^* > 0$ and $\sigma_1^* > 0$ such that $k_\gamma^* + F_\gamma\theta_{\gamma 1} - \frac{1}{2}\sigma_1^*(1+F_\gamma\theta_{\gamma 1}) > 0$, $1-\frac{1}{2}\sigma_1^{*-1}(1+F_\gamma\theta_{\gamma 1}) > 0$ by Assumption 1. Therefore, there exist $k_\gamma > k_\gamma^*$ and $\sigma_1 > \sigma_1^*$ satisfying $\Delta_3 > 0$ and $\Delta_4 > 0$. Additionally, since $(\Delta_1, \Delta_2, \Delta_3, \Delta_4)$ are independent of σ_2, there exists $\sigma_2^* > 0$ such that $\Delta_5 > 0$ for $\sigma_2 > \sigma_2^*$. Then it can be directly concluded that the value of σ_2, which ensures $\Delta_5 > 0$, could simultaneously ensure $\Delta_6 > 0$ and $\Delta_7 > 0$, because $\Delta_6 = \sigma_2 k_{\alpha-q}\Delta_5/2$ and $\Delta_7 = \Delta_5\sigma_2^2\Delta_5/4$. Finally, there exists $\sigma_\eta^* > 0$ such that Δ_8 are positive when $\sigma_\eta > \sigma_\eta^*$, for $\Delta_i (i = 1, 2, \cdots, 7)$ are independent of σ_η. Therefore, the matrix $\mathbf{P}$ can be made positive-definite by proper selection of these parameters. It then follows that all states of (40) and (41) remain bounded and $\lim_{t\to\infty}\tilde{\boldsymbol{x}} = \mathbf{0}$ by Barbalat's lemma, which completes the proof.

4 Simulation

To evaluate the proposed control system, a series of simulations are presented in this section. First, the control law is tested on the nominal AHSV model, serving as the baseline for the subsequent comparison. Then, parameter uncertainty is considered for robustness verification. A step-velocity increment of 1000ft/s and an altitude increment of 10000ft from the initial are used as the command. Notice that as [10], the step commands have been filtered to generate the reference trajectories of the velocity and altitude through a second-order prefilter.

The first simulation will test the proposed control law on the nominal AHSV model. Precise tracking of the altitude and velocity reference trajectories, as well as rapid regulation of angle of attack to the desired point is observed in Fig. 2, which is the basic objective of the AHSV control system. Stable and damped behaviors of the flexible states $\boldsymbol{\eta}$ are shown in Fig. 3

Parameter uncertainty is introduced in the following simulations to illustrate the robustness of the proposed control system. Two most common uncertainties in AHSV dynamics are considered here. One is the uncertainty of the aerodynamic coefficients, and the other is the structure parameter variation due to fuel consumption. For the aerodynamic coefficients, a maximum variation within 30% of the nominal has been considered. The structure parameter variation due to fuel consumption reported in Table 1of [19] has been used here, which presents different structure parameters corresponding to the 0%, 30%, 50%,70% and 100% fuel level respectively. Simulation results are shown in Fig. 4 and Fig. 5. It is observed that in each case the tracking errors of the velocity, altitude and angle of attack remain small during the entire maneuver and vanish asymptotically.

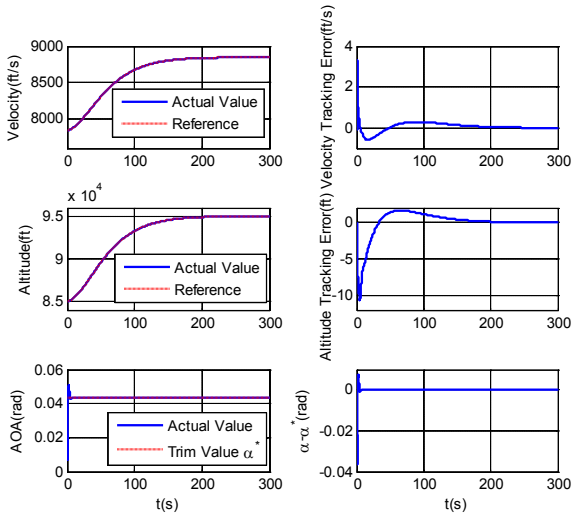

Fig. 2. Velocity, altitude and angle of attack tracking performance

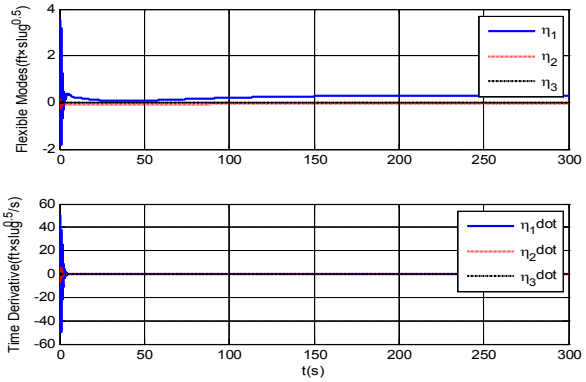

Fig. 3. Time histories of flexible modes and their time derivative

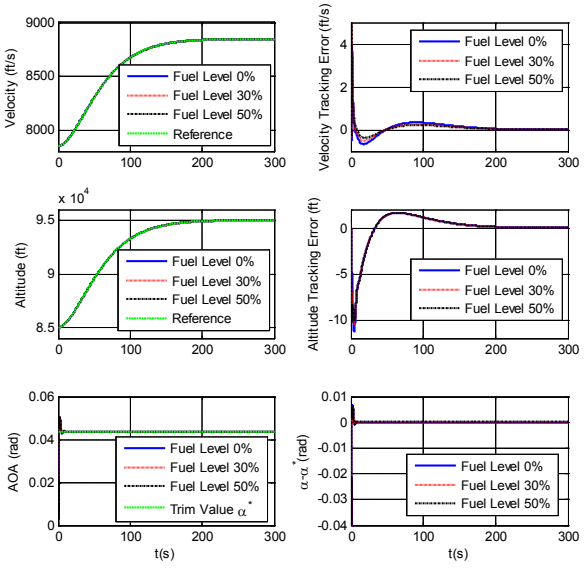

Fig. 4. Velocity, altitude and angle of attack tracking performance ((fuel level 0%, 30% and 50%)

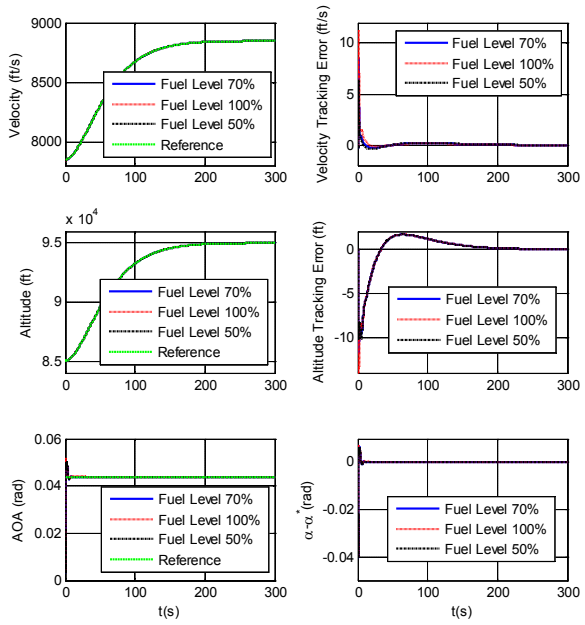

Fig. 5. Velocity, altitude and angle of attack tracking performance ((fuel level 70%, 100% and 50%)

5 Conclusion

In this paper an adaptive immersion and invariance based control system is designed for a non-minimum phase hypersonic vehicle model with parameter uncertainty. The architecture of the whole control system is constructed by decomposing the vehicle dynamics into three parallel subsystems, namely the velocity, altitude/flight-path angle, and angle of attack/pitch rate subsystems, where I&I based estimators are applied to estimate the unknown parameters of each subsystem on-line. Notably the flexible effects on the rigid dynamics are considered in controller synthesis. Representative simulations are conducted and the results illustrate the effectiveness and robustness of the proposed control system.

References

[1] B. Fidan, M. Mirmirani, and P. Ioannou, "Flight dynamics and control of air-breathing hypersonic vehicles: review and new directions," in *Proc. AIAA international space planes and hypersonic systems and technologies*, Norfolk, VA, 2003, AIAA 2003-7081.

[2] D. B. Doman, M. W. Oppenheimer, and M. A. Bolender, "Progress in guidance and control research for space access and hypersonic vehicles," in *Proceedings of IEEE Conference on Decision and Control,* San Diego, CA, 2006, pp. 6837-6851.

[3] M. Mirmirani, C. Wu, A. Clark, S. Choi, and R. Colgren, "Modeling for control of a generic airbreathing hypersonic vehicle," in *Proc. AIAA Navigation and Control Conference and Exhibit*, California, 2005, AIAA 2005-6256.

[4] Q. Zong, F. Wang, B. Tian, and R. Su, "Robust adaptive dynamic surface control design for a flexible air-breathing hypersonic vehicle with input constraints and uncertainty," *Nonlinear Dyn.*, vol. 78, no. 1, pp. 289–315, Oct. 2014.

[5] X. X. Hu, C. H. Hu, L. G. Wu, H. J. Gao, "Output tracking control for nonminimum phase flexible air-breathing hypersonic vehicle models," *J. Aerosp. Eng*, vol. 28, no. 2, pp. 1-11, Mar. 2015.

[6] E. Mooij, "Numerical investigation of model reference adaptive control for hypersonic aircraft," *J. Guid. Control Dyn.,* vol. 24, no. 2, pp. 315–323, Mar.-Apr. 2001.

[7] D. O.Sigthorsson, P. Jankovsky, A. Serrani, S. Yurkovich, M. A. Bolender and D. B. Doman, "Robust linear output feedback control of an airbreathing hypersonic vehicle," *J. Guid. Control Dyn.,* vol. 31, no. 4, pp. 1052–1066, Jul.-Aug. 2008.

[8] H. Xu, M. Mirmirani, and P. Ioannou, "Adaptive sliding mode control design for a hypersonic flight vehicle," *J. Guid. Control Dyn.,* vol. 27, no. 5, pp. 829–838, Sep.-Oct. 2004.

[9] Y. B. Liu, D. B. Xiao, and Y. P. Lu, "Research on advanced flight control methods based on actuator constraints for elastic model of hypersonic vehicle," *Proc IMechE Part G: Journal of Aerospace Engineering,* vol.228, no. 9, pp. 1627-1637, Apr. 2014.

[10] L.Fiorentini, A. Serrani, M. A. Bolender, and D. B. Doman, "Nonlinear robust adaptive control of flexible air-breathing hypersonic vehicles," *J. Guid. Control Dyn.,* vol. 32, no. 2, pp. 401–416, Mar.-Apr. 2009.

[11] B. Xu, F. Sun, C. Yang, D. Gao, and J. Ren, "Adaptive discrete-time controller design with neural network for hypersonic flight vehicle via back-stepping," *Int. J. Control*, vol. 84, no. 9, pp. 1543-1552, Sep. 2011.

[12] A. B. Waseem, Y. Lin, and A. S. Kendrick, "Adaptive integral dynamic surface control of a hypersonic flight vehicle," *Int. J. Syst. Sci.*, vol. 46, no. 10, pp. 1717–1728, 2015.

[13] Q. Zong, F. Wang, B. Tian, and J. Wang. [2014, Aug.] Robust Adaptive Approximate Backstepping Control Design for a Flexible Air-breathing Hypersonic Vehicle. *J. Aerosp. Eng,* vol. 28, no. 4, pp. 1-16, Jul. 2015.

[14] A. Astolfi, D. Karagiannis, and R. Ortega, *Nonlinear and Adaptive Control with Applications*, London: Springer, 2008.

[15] C. Hu and Y. Liu, "Nonlinear adaptive equivalent control based on interconnection subsystems for air-breathing hypersonic vehicles," *Journal of applied mathematics*, vol. 2103, pp. 1-10, 2013.

[16] M. Chen, B. Ren, Q. X. Wu, and C. S. Jiang, "Anti-disturbance control of hypersonic flight vehicles with input saturation using disturbance observer," *Sci China Inf Sci*, vol. 58, no. 7, pp. 1-12, July 2015.

[17] J. Yang, S. H. Li, C. Y. Sun, and L. Guo, "Nonlinear-disturbance-observer-based robust flight control for airbreathing hypersonic vehicles," *IEEE Trans Aerosp Electron Syst,* 2013; 49(2): 1263–1275.

[18] M. A. Bolender and D. B. Doman, "Nonlinear longitudinal dynamical model of an sir-breathing hypersonic vehicle," *J. Spacecraft Rockets*, vol. 44, no. 2, pp. 374-387, March-April 2007.

[19] D. O.Sigthorsson, P. Jankovsky, A. Serrani, S. Yurkovich, M. A. Bolender and D. B. Doman, "Robust linear output feedback control of an airbreathing hypersonic vehicle," *J. Guid. Control Dyn.,* vol. 31, no. 4, pp. 1052–1066, Jul.-Aug. 2008.